

Top quark production near threshold: NNLO QCD correction

Oleg Yakovlev^{1,a}

¹ *Institut für Theoretische Physik,
Universität Würzburg, D-97074 Würzburg, Germany*

Abstract

We consider the process $e^+e^- \rightarrow t\bar{t}$ near threshold with NNLO accuracy by using two alternative approaches. The NNLO correction turns out to be of the same order as the NLO correction. The obtained results are compared with the existing results in the literature. Our final results obtained in one approach are in agreement with [12] but the results obtained in another approach differ numerically from [13].

PACS numbers: 12.38.Bx, 12.38.Cy, 13.85.Lg, 14.65.Ha

to be submitted in Phys. Lett. B

^ae-mail: iakovlev@physik.uni-wuerzburg.de

1. Introduction.

A detailed study of the process $e^+e^- \rightarrow t\bar{t}$ will be performed at the Next Linear Collider [1]. As a result of this study the precision measurements of the top quark mass m and width Γ and of the QCD coupling constant $\alpha_s(m)$ can be done at NLC.

The cross section of the top quark production at LO and NLO was studied in detail in [2, 3, 5, 6, 7]. The general approach for the calculation of the cross section $e^+e^- \rightarrow t\bar{t}$ was developed in [2]. There it was pointed out that the large width of the top quark serves as a cutoff for long-distance effects in this problem. Because of that reliable predictions for the cross section can be obtained by using perturbative QCD. It is well known that the standard QCD perturbation theory does not work in the threshold region. Even at LO approximation one has to resum all $(\alpha_s/v)^N$ terms. The result of such resummation is proportional to the nonrelativistic Coulomb Green function at the origin. At NLO and NNLO one has to resum all $(\alpha_s/v)^N(1, \alpha_s, v, \alpha_s^2, \alpha_s v, v^2)$ terms in order to calculate the cross section in the threshold region.

The approach to the NNLO calculations was suggested in [8] and consists of two steps. First, one calculates the cross section in NNLO order far from the threshold, in the region $\alpha_s \ll v \ll 1$, ($v = \sqrt{1 - 4m^2/s}$ is the relative velocity of top quark and antiquark), where the resummation of the Coulomb singularities is not needed. Then one considers the nonrelativistic cross section using an infrared cutoff, and matches it with the cross section in the region $\alpha_s \ll v \ll 1$.

The Abelian part of the corrections to the cross section near threshold, proportional to the structures C_F^2 and $C_F T N_L$ were calculated in [8] and [9] respectively. The complete NNLO correction to the cross section for from the threshold, in the region $\alpha_s \ll v \ll 1$, was calculated in [10, 11]. The NNLO correction to the cross section of top production near threshold was considered recently in two papers [12] and [13] by using two alternative approaches. The difference of the numerical results between [12] and [13] is expected to be small, but actually the difference is large and amounts to 5 – 15%.

The main purpose of this Letter is to calculate the cross section of the process $e^+e^- \rightarrow t\bar{t}$ with NNLO accuracy in the energy region close to the threshold by using two alternative approaches and to clarify the origin of the difference between [12] and [13].

Our final results obtained in one approach are in agreement with [12] but results obtained in another approach differ numerically by about 5 – 10% from [13].

The paper is organized as follows. In section 2 we discuss basic elements needed to calculate the NNLO cross section. In section 3 we consider the matching procedure and fix the short distance coefficient. In section 4 we present the final formula for the cross section, and results of the numerical analysis.

2. Basic elements of R_{NNLO} .

The cross section of the process $e^+e^- \rightarrow t\bar{t}$ in the near threshold region can be obtained by using the optical theorem and an expansion of the vector current $\bar{t}\gamma_\mu t$. The cross section reads

$$R = \sigma(e^+e^- \rightarrow t\bar{t})/\sigma_{pt} = e_Q^2 N_c \frac{24\pi}{s} C(r) \text{Im} \left[\left(1 - \frac{\vec{p}^2}{3m^2}\right) G(r, r|E + i\Gamma) \right] \Big|_{r \rightarrow 0}, \quad (1)$$

where $\sigma_{pt} = 4\pi\alpha^2/3s$, e_Q is the electric charge of the top quark, N_c is the number of colors, $\sqrt{s} = 2m + E$ is the total energy of the quark antiquark system, m is the top quark pole mass, Γ is the top quark width. $G(\vec{r}, \vec{r}'|E + i\Gamma)$ is the nonrelativistic Green function, which satisfies to the Schrödinger equation

$$(H - E - i\Gamma)G(\vec{r}, \vec{r}'|E + i\Gamma) = \delta(\vec{r} - \vec{r}'). \quad (2)$$

The Green function is divergent at the origin $r \rightarrow 0$ because the potential contains $1/r^2$ terms. These singularities are regularized and factorized to the short distance coefficient $C(r_0)$.

In eq.(1) we have already used a complex energy, $E + i\Gamma$, in the Green function, according to [2]. This structure appears in the top quark propagator through the top quark self energy at LO, NLO and NNLO. The non-factorizable corrections were studied at NLO in [7, 14, 6]. It was shown that they cancel in the total cross section. It was argued in [15] that the cancellation appears in all α_s orders. Therefore we do not consider nonfactorizable corrections here .

2a. Hamiltonian and QCD potential.

The nonrelativistic Hamiltonian of the heavy quark antiquark system reads

$$H = H_0 + W(r), \quad H_0 = \frac{\vec{p}^2}{m} + V(r), \quad (3)$$

here $V(r)$ is a static QCD potential of the heavy quark-antiquark system at NNLO order:

$$\begin{aligned} V(r) = & -\frac{C_F\alpha_s}{r} \left(1 + \frac{C_F\alpha_s}{4\pi} (2\beta_0 \ln(\mu_1 r) + a_1) \right) \\ & + \frac{\alpha_s}{4\pi} \left(\beta_0^2 (4 \ln^2(\mu_1 r) + \frac{\pi^2}{3}) + 2(\beta_1 + 2\beta_0 a_1) \ln(\mu_1 r) + a_2 \right), \end{aligned} \quad (4)$$

here $\mu_1 = \mu_s e^\gamma$, μ_s is the normalization scale, γ is the Euler constant, $\alpha_s = \alpha_s(\mu_s)$.

The coefficients a_1 and a_2 were calculated in [16, 17], respectively

$$\begin{aligned} a_1 = & \frac{31}{9}C_A - \frac{20}{9}T_R N_L, \\ a_2 = & \left(\frac{4343}{162} + 6\pi^2 - \frac{\pi^4}{4} + \frac{22}{3}\zeta_3 \right) C_A^2 - \left(\frac{1798}{81} + \frac{56}{3}\zeta_3 \right) C_A T_R N_L \\ & + \left(\frac{20}{9}T_R N_L \right)^2 - \left(\frac{55}{3} - 16\zeta_3 \right) C_F T_R N_L. \end{aligned} \quad (5)$$

We also take into account the first two coefficients in the expansion of the QCD β -function

$$\beta_0 = \frac{11}{3}C_A - \frac{4}{3}N_L T_R, \quad \beta_1 = \frac{34}{3}C_A^2 - \frac{20}{3}C_A T_R N_L - 4C_F T_R N_L. \quad (6)$$

The color factors are $C_F = 4/3$, $C_A = 3$, $T_R = 1/2$. $N_L = 5$ is the number of light quarks.

2b. Breit-Fermi Hamiltonian.

The function $W(r)$ in eq.(3) is the QCD generalization of the QED Breit-Fermi Hamiltonian [18, 19]. We consider here quark antiquark production in the S -wave mode. The Breit-Fermi Hamiltonian for the final state with $\vec{L} = 0, \vec{S}^2 = 2$ reads [18, 19]

$$W(r) = -\frac{\vec{p}^4}{4m^3} + \frac{11\pi C_F \alpha_s}{3m^2} \delta(\vec{r}) - \frac{C_F \alpha_s}{2m^2} \left\{ \frac{1}{r}, \vec{p}^2 \right\} - \frac{C_A C_F \alpha_s^2}{2mr^2}. \quad (7)$$

Let us demonstrate how the Breit-Fermi Hamiltonian can be reduced to a convenient form for the numerical and analytical evaluation. First we note that eq. (7) can be rewritten in the following way

$$W(r) = -\frac{H_0^2}{4m} + \frac{3}{4m} \{V_0(r), H_0\} + \frac{11\pi C_F \alpha_s}{3m^2} \delta(\vec{r}) - \left(\frac{5}{2} + \frac{C_A}{C_F} \right) \frac{V_0^2(r)}{2m}. \quad (8)$$

Here we used $V_0(r) = -\frac{C_F \alpha_s}{r}$. The first and second terms in eq.(8) can be simplified by using equation of motion, $(H - \bar{E})G(r', r''|\bar{E}) = \delta(r' - r'')$, $\bar{E} = E + i\Gamma$, but the third and fourth terms are related by the commutation relation

$$[H_0, ip_r] = \frac{4\pi\delta(\vec{r})}{m} - \frac{C_F \alpha_s}{r^2}, \quad (9)$$

with $ip_r = \frac{1}{r} \frac{\partial}{\partial r} r$. Expressing the term with $1/r^2$ through $\delta(\vec{r})$ function and using the commutation relations, we have (assuming $r \rightarrow 0$)

$$\begin{aligned} G^{NNLO}(r, r|\bar{E}) &= \left(1 + \frac{\bar{E}}{2m}\right) G_C^{NNLO}(r, r|\bar{E} + \frac{\bar{E}^2}{4m}) \Big|_{\alpha_s \rightarrow \alpha_s(1 + \frac{3\bar{E}}{2m})} \\ &+ \frac{4\pi C_F \alpha_s}{3m^2} \left(1 + \frac{3C_A}{2C_F}\right) \left[G_C^{LO}(r, r|\bar{E})\right]^2. \end{aligned} \quad (10)$$

We have omitted some unimportant surface terms above. Here $G_C(r, r|E)$ is the Green function calculated only with the Coulomb potential and without the Breit-Fermi Hamiltonian. The LO Green function can be presented in the form [8] ($v = \sqrt{\frac{E}{m}}$)

$$G_C^{LO}(0, 0|\bar{E}) = \frac{m^2}{4\pi} \left(iv - C_F \alpha_s \left(\log\left(\frac{imv}{\mu_f}\right) + \gamma_E + \Psi\left(1 - i\frac{C_F \alpha_s}{2v}\right) \right) \right), \quad (11)$$

here μ_f is a factorization scale, which disappears in R after performing a matching procedure. Employing this form of the LO Green function, we get the $NNLO$ Green function in the form

$$\begin{aligned} G^{NNLO}(0, 0|\bar{E}) &= G_C^{NNLO}(0, 0|\bar{E}) - G_C^{LO}(0, 0|\bar{E}) \\ &+ \frac{4\pi C_F \alpha_s}{3m^2} \left(1 + \frac{3C_A}{2C_F}\right) \left[G_C^{LO}(0, 0|\bar{E})\right]^2 + \frac{m^2}{4\pi} \left(iv \left(1 + \frac{5}{8} v^2\right) \right. \\ &- \left. \alpha_s C_F (1 + 2v^2) \left(\log\left(\frac{-imv}{\mu_f}\right) + \gamma_E + \Psi\left(1 - i\frac{C_F \alpha_s}{2v} \left(1 + \frac{11}{8} v^2\right)\right) \right) \right). \end{aligned} \quad (12)$$

Equations (10) and (12) are in agreement with [12] but they are obtained in a different way. Expanding eq.(10) in $\alpha_s^2, v\alpha_s, v^2$ we have

$$\begin{aligned}
G^{NNLO}(0, 0|\bar{E}) &= G_C^{NNLO}(0, 0|\bar{E}) + \delta(G)_1 + \delta(G)_2 \quad (13) \\
\delta(G)_1 &= \frac{im^2v}{4\pi} \left(\frac{5}{8}v^2 + \frac{11}{16}(\alpha_s C_F)^2 \Psi'(1 - i\frac{C_F\alpha_s}{2v}) \right. \\
&\quad \left. + iv2C_F\alpha_s(\log(\frac{imv}{\mu_f}) + \gamma_E + \Psi(1 - i\frac{C_F\alpha_s}{2v})) \right), \\
\delta(G)_2 &= \frac{4\pi C_F\alpha_s}{3m^2} \left(1 + \frac{3C_A}{2C_F} \right) [G_C^{LO}(0, 0|\bar{E})]^2.
\end{aligned}$$

These expressions are our analytical results for the correction to the Green function at the origin.

An alternative strategy (adopted also in [13]) is to keep the Breit-Fermi correction together with the QCD potential in Schrödinger equation and to solve the Schrödinger equation numerically. The main reason for doing that is, that, the expansion procedure can be not safe for energy denominators of the Green function

$$G(r, r|E) = \sum_n \frac{\psi_n^2(r)}{E_n - E - i\Gamma} + \int \frac{dk}{2\pi} \frac{\psi_k^2(r)}{E_k - E - i\Gamma} \quad (14)$$

especially if the energy is close to the energy of resonant state.

Therefore, we reexpress the $\delta(\vec{r})$ function in eq.(8) by the term with $1/r^2$ by using the commutation relation (9)

$$W(r) = -\frac{H_0^2}{4m} + \frac{3}{4m} \{V_0(r), H_0\} + \frac{11\alpha_s C_F}{12m} [H_0, ip_r] - \left(\frac{2}{3} + \frac{C_A}{C_F} \right) \frac{V_0^2(r)}{2m}. \quad (15)$$

We consider the first correction to the Green function $G(r', r''|\bar{E})$ originated from $W(r)$. Using the equation of motion we obtain

$$\begin{aligned}
- \int d\vec{r} G(r', r|\bar{E}) W(r) G(r, r''|\bar{E}) &= \left(\frac{\vec{p}^2}{2m^2} + \frac{\alpha_s C_F}{mr'} + ip_r \frac{11\alpha_s C_F}{12m} \right) G(r', r''|\bar{E}) + \quad (16) \\
&\int d\vec{r} G(r', r|\bar{E}) \left[\frac{\bar{E}^2}{4m} - \frac{3V_0\bar{E}}{2m} + \left(\frac{2}{3} + \frac{C_A}{C_F} \right) \frac{V_0^2(r)}{2m} \right] G(r, r''|\bar{E}).
\end{aligned}$$

The surface term with ip_r does not coincide with the one from [13]. We see from the second line of the eq.(16) that the problem of evaluating the Breit-Fermi correction is reduced to solving the following equation

$$(H_1 - E_1)G_1(r, r'|E_1) = \delta^3(r - r'), \quad (17)$$

with new energy $E_1 = \bar{E} + \frac{\bar{E}^2}{4m}$ and with new Hamiltonian

$$H_1 = \frac{\vec{p}^2}{m} + V(r) + \frac{3V_0\bar{E}}{2m} - \left(\frac{2}{3} + \frac{C_A}{C_F} \right) \frac{V_0^2(r)}{2m}. \quad (18)$$

The numerical solution of (17) gives us the Green function at NNLO order.

3. Matching procedure.

Now we consider the matching procedure in order to fix the short distance coefficient $C(r)$ in eq.(1). First we calculate the first-order correction to the Green function originated from $W(r)$. This is given by the following integral

$$- \int d^3r G_0(r_0, r|\bar{E})W(r)G_0(r, r_0|\bar{E}) \quad (19)$$

with the free Green function ($k = mv$)

$$G_0(r, r'|\bar{E}) = \frac{m}{4\pi} \left(\frac{\sin(kr)}{k} e^{ikr'} \theta(r' - r) + \frac{\sin(kr')}{k} e^{ikr} \theta(r - r') \right). \quad (20)$$

Then we compare the result of this integration with the NNLO QCD radiative correction to the cross section $e^+e^- \rightarrow t\bar{t}$ in the region $\alpha_s \ll v \ll 1$ [10]. Iterations of the Coulomb potential give only terms proportional to $1/v, 1/v^2$ at NNLO in this kinematical region. These terms are trivially identified in R . We obtain the following short distance correction

$$C(r) = 1 - \frac{C_F \alpha_s(\mu_h)}{\pi} + C_2(r) \left(\frac{C_F \alpha_s(\mu_h)}{4\pi} \right)^2, \quad (21)$$

$$C_2(r) = A_1 \log(r/a) + A_2 \log(m/\mu_h) + A_3 \quad (22)$$

with

$$A_1 = \pi^2 \left(C_A + \frac{2C_F}{3} \right), \quad a = \frac{e^{2-\gamma_E}}{2m}, \quad A_2 = 2\beta_0, \quad (23)$$

$$A_3 = C_F C_2^A + C_A C_2^{NA} + T_R N_L C_2^L + T_R N_H C_2^H, \quad (24)$$

with

$$\begin{aligned} C_2^A &= \frac{39}{4} - \zeta_3 + \pi^2 \left(\frac{4}{3} \ln 2 - \frac{35}{18} \right), \\ C_2^{NA} &= -\frac{151}{36} - \frac{13}{2} \zeta_3 + \pi^2 \left(\frac{179}{72} - \frac{8}{3} \ln 2 \right), \\ C_2^H &= \frac{44}{9} - \frac{4}{9} \pi^2, \\ C_2^L &= \frac{11}{9}. \end{aligned} \quad (25)$$

Here μ_h is the hard normalization scale. We should note that matching of the analytical expressions of the eqs.(10)-(13) gives similar results but with substitution $r/a \rightarrow m/\mu_f$. These coefficients are in agreement with results obtained in [8, 12, 13].

4. Numerical results.

The final expression for the NNLO cross section is given by the following equation

$$R_{NNLO}(E) = \left(1 - \frac{C_F \alpha_s}{\pi} + C_2(r_0) \left(\frac{C_F \alpha_s}{4\pi} \right)^2 \right) \frac{8\pi}{m^2} \text{Im} \left(\left(1 - \frac{5\bar{E}}{6m} \right) G_1(r_0, r_0|E_1) \right), \quad (26)$$

with $G_1(r_0, r_0|E_1)$ being solution of the eqs.(17)-(18) and with $C_2(r_0)$ from (21)-(25). The analytical result for R_{NNLO} is given by the same formula (26) with $G(0, 0|\bar{E})$ from eqs.(10)-(13) and with substitutions: $r \rightarrow ma/\mu_f$ in $C(r)$ and $(1 - \frac{5\bar{E}}{6m}) \rightarrow (1 - \frac{4\bar{E}}{3m})$ in eq.(26).

In order to solve the Shrödinger equation numerically we have written two programs in FORTRAN and MATHEMATICA. We have checked that the programs reproduce the results of the analytical expression for the Green function in the pure Coulomb problem and numerical values for NLO cross section from [12, 13]. The results of both programs for the NNLO correction give the same result. Therefore we are confident in our numerical results.

The Fig.1 shows our final results for $R_{NNLO}(E)$ as a function of the nonrelativistic energy $E = \sqrt{s} - 2m$. We compare the NNLO results with LO and NLO curves, for the soft scale $\mu_s = 50, 75, 100$ GeV. We have chosen $m = 175 GeV$, $\Gamma = 1.43 GeV$, $r_0 = a$ and $\alpha_s(M_Z) = 0.118$. We see that NNLO correction is of the order 20% and as large as NLO one. The $1S$ peak is shifted towards smaller energies. The dependence of the NNLO cross section on the parameter μ_s is better then in LO, but worse than in NLO.

The dependences on the factorization scale r_0 and hard normalization scale μ_h are much smaller then on μ_s . We demonstrate that fact in Fig 2., where we plot $R_{NNLO}(E)$ as a function of energy at $r_0 = 2a, a, a/2$. In Fig.3 we show $R_{NNLO}(E)$ at $\mu_h = 2m, m, m/2$. In Fig.4 we demonstrate $R_{NNLO}(E)$ at different $\alpha_s(M_Z) = 0.116, 0.118, 0.12$. We see that $R_{NNLO}(E)$ is very sensitive to the value of the QCD coupling $\alpha_s(M_Z)$. Comparing our results (Fig.1) with the numerical results of [13] we have found that they differ by about 5 – 10%. However, if we adopt the approach of [12] and expand the Green function in the Breit-Fermi Hamiltonian we obtain the results that are in agreement with results presented in [12], see eqs. (10)-(13). The results obtained by the two methods turn out to be closer numerically to each other than the results of [12] and [13].

5. Conclusion and outlook.

In conclusion, we have calculated the total cross section of the top quark production with NNLO accuracy. The NNLO correction is of the same order as the NLO. The comparison of obtained results with the results published in [12, 13] shows that our final results are in agreement with [12] and differ numerically from that of [13].

Finally, let us mention some open questions in this field. It is quite important to consider NNLO correction to the total cross section in the scheme with the running QCD coupling α_s and in the scheme with the low-scale running top quark mass, for example $m_{PS}(\mu)$ [20]. It would be interesting in future to examine the size of the NNLO corrections to the differential distributions, for example to the distribution over spatial momentum, $\frac{d\sigma}{d|\vec{p}_{t\bar{t}}|}$. It is necessary to analyze nonfactorizable corrections to the differential cross section at NNLO. In view of the fact that NNLO correction is large it would be useful to check NNLO correction to the static QCD potential, the coefficient a_2 [17].

Acknowledgements.

I am grateful to A. Khodjamirian, R. Rückl for discussions and comments. This work is supported by the German Federal Ministry for Research and Technology (BMBF) under contract number 05 7WZ91P (0).

References

- [1] E. Accomando *et al.*, the ECFA/DESY LC Physics Working Group, *Physics with e^+e^- linear colliders*, DESY 97-100, hep-ph/9705442.
- [2] V.S. Fadin and V.A. Khoze, JETP Lett. **46** (1987), 525;
Sov. J. Nucl. Phys. **48** (1988), 309.
- [3] M. Peskin and M. Strassler, Phys. Rev. **D43** (1991), 1500.
- [4] W. Kwong, Phys. Rev. **D43** (1991), 1488.
- [5] M. Jeřabek, J.H. Kuhn and T. Teubner, Z. Physik **C56** (1992), 653;
Y. Sumino, K. Fujii, K. Hagiwara, H. Murayama and C.-K. Ng,
Phys. Rev. **D47** (1993), 56.
- [6] Y. Sumino, Ph.D thesis, Tokyo, 1993;
- [7] K. Melnikov and O. Yakovlev, Phys. Lett. **B324** (1994), 217.
- [8] A.H. Hoang, Phys. Rev. **D56** (1997), 5851.
- [9] A.H. Hoang, J. H. Kuhn and T. Teubner, Nucl. Phys. **B 452** (1995) 173.
- [10] A. Czarnecki and K. Melnikov, Phys. Rev. Lett. **80** (1998) 2531.
- [11] M. Beneke and V. A. Smirnov, Nucl. Phys. **B522** (1998) 321
M. Beneke, A. Signer and V.A. Smirnov, Phys. Rev. Lett. **80** (1998) 2535.
- [12] A.H. Hoang and T. Teubner, preprint UCSD/PTH 98-01,
DESY 98-008, hep-ph/9801397.
- [13] K. Melnikov and A. Yelkhovsky, Nucl. Phys. **B528** (1998) 59.
- [14] V.S Fadin, V.A. Khoze, A.D. Martin, Phys. Rev. **D49** (1994), 2247.
- [15] V.S Fadin, V.A. Khoze, A.D. Martin, Phys. Lett. **B320** (1994), 141.
- [16] W. Fischler, Nucl. Phys. **B129** (1977), 157;
A. Billoire, Phys. Lett. **B92** (1980), 343.
- [17] M. Peter, Nucl. Phys. **B501** (1997), 471.
- [18] L.D. Landau and E.M. Lifschitz, *Relativistic Quantum Theory*,
part 1 (Pergamon, Oxford, 1974).
- [19] S.N. Gupta and S.F. Randford, Phys. Rev. **D24** (1981), 2309,
(E) *ibid* **D25** (1982), 3430;
S.N. Gupta, S.F. Randford and W.W. Repko, Phys. Rev. **D26** (1982), 3305.
- [20] M. Beneke, preprint CERN-TH/98-120, hep-ph/9804241.

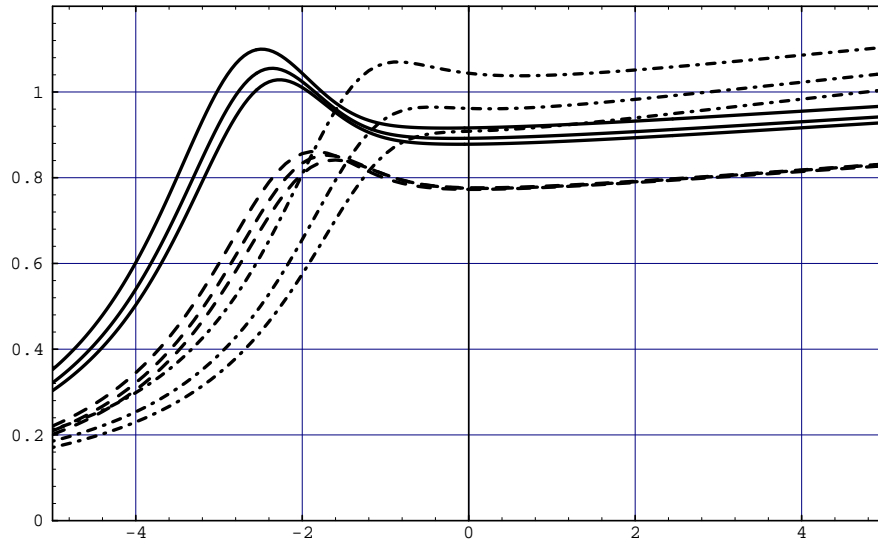


Figure 1: $R(e^+e^- \rightarrow t\bar{t})$ for the LO (dashed-dotted lines), NLO (dashed lines), NNLO (solid lines) approximation as a function of energy $E = \sqrt{s} - 2m$, GeV. In all cases we use $m_t = 175$ GeV, $\Gamma_t = 1.43$ GeV, $\alpha_s(m_Z) = 0.118$ but different values of the soft scale $\mu_s = 50, 75, 100$ GeV.

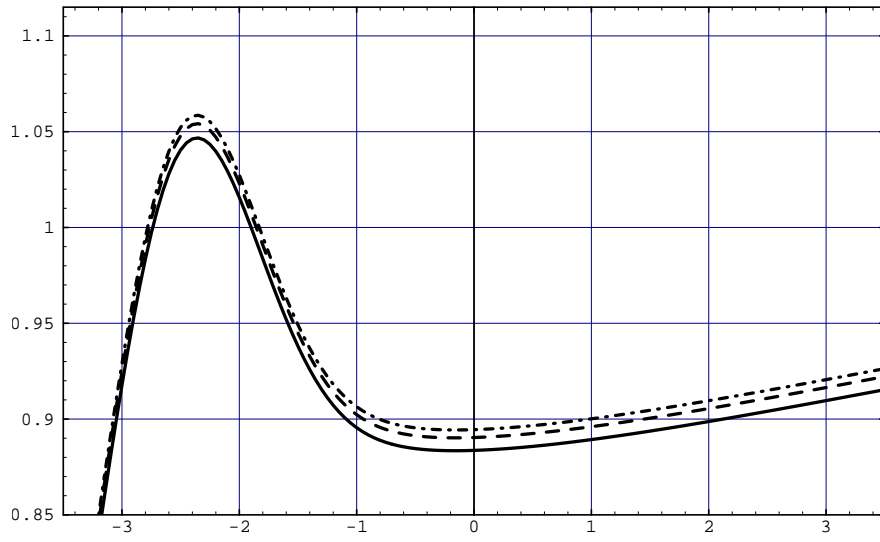


Figure 2: $R(e^+e^- \rightarrow t\bar{t})$ at NNLO at different values of factorization scale $r_0 = 2a$ (dashed-dotted line), $r_0 = a$ (dashed line) and $r_0 = a/2$ (solid line). We use $m_t = 175$ GeV, $\Gamma_t = 1.43$ GeV, $\mu_s = 75$ GeV, $\alpha_s(m_Z) = 0.118$.

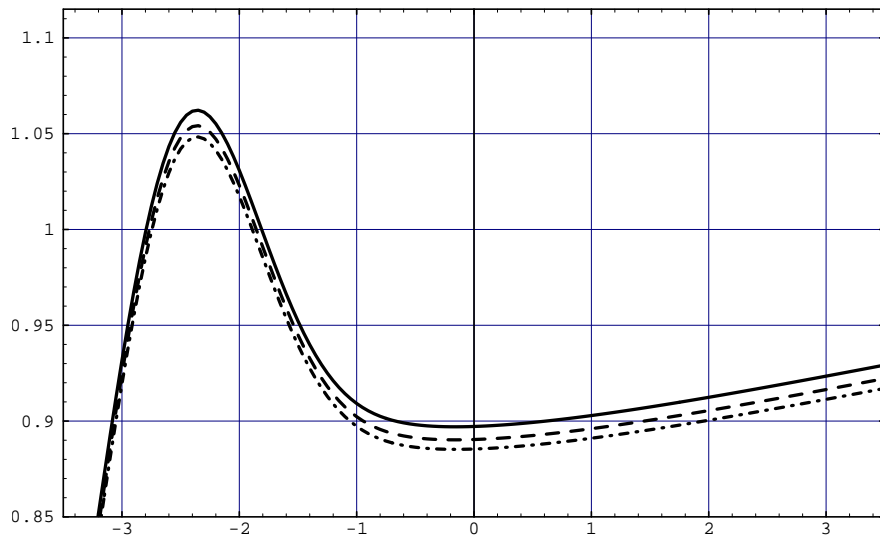


Figure 3: $R(e^+e^- \rightarrow t\bar{t})$ at NNLO at different value of the hard normalization scale $\mu_h = 2m$ (dashed-dotted line), $\mu_h = m$ (dashed line) and $\mu_h = m/2$ (solid line). We use $m_t = 175 \text{ GeV}$, $\Gamma_t = 1.43 \text{ GeV}$, $\mu_s = 75 \text{ GeV}$, $\alpha_s(m_Z) = 0.118$.

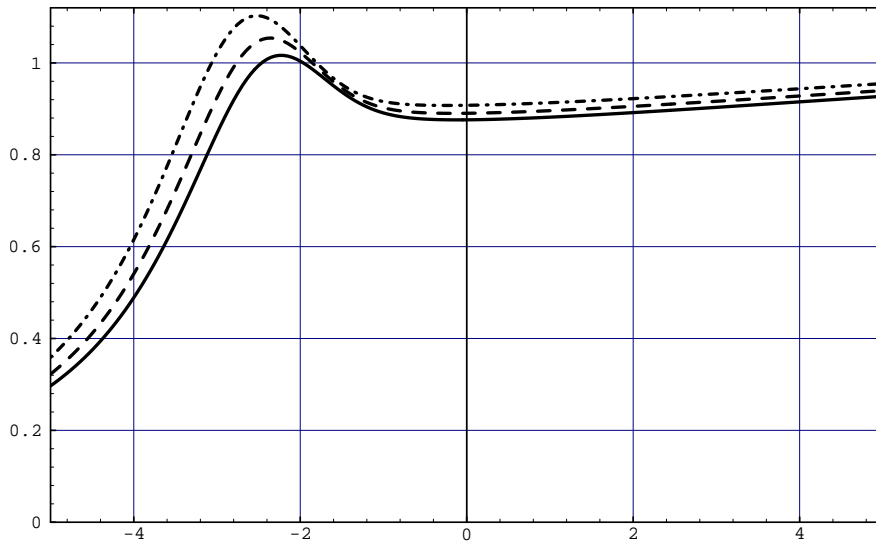


Figure 4: $R(e^+e^- \rightarrow t\bar{t})$ at NNLO at different values of the QCD coupling constant $\alpha_s(m_Z) = 0.116$ (solid line), $\alpha_s(m_Z) = 0.118$ (dashed line), $\alpha_s(m_Z) = 0.120$ (dashed-dotted line). We use $m_t = 175$ GeV, $\Gamma_t = 1.43$ GeV and $\mu_s = 75$ GeV.